Epitaxial Growth, Processing and Characterization of Semiconductor Nanostructures

Borgström, Magnus

2003

ELSEVIER

Applied Surface Science 165 (2000) 241–247

applied surface science

www.elsevier.nl/locate/apsusc

Effects of substrate doping and surface roughness on self-assembling InAs/InP quantum dots

M. Borgström*, J. Johansson, L. Landin, W. Seifert

Solid State Physics, University of Lund, Box 118, S-221 00 Lund, Sweden

Received 25 January 2000; accepted 8 June 2000

Abstract

The effect of substrate doping (InP:Sn and InP:Fe) and surface morphology of InP (001), misoriented 0.2° off towards ⟨110⟩, on densities and sizes of self-assembled InAs quantum dots was investigated. The dots were deposited on either well-defined terraced surfaces with monolayer high steps grown at 650°C in the step–flow growth mode, or on more rough InP surfaces prepared at a lower temperature of 500°C. The dot densities were found to vary between 0.5×10^{10} $cm^{-2} < \rho < 4.0 \times 10^{10}$ cm^{-2} with otherwise identical growth conditions. The dot densities were lower on terraced surfaces and on Sn-doped substrates in comparison to the rougher surface and on Fe-doped substrates. This very broad scattering of densities indicates that InAs island formation on InP substrates is very sensitive to the choice of substrates and substrate preparation.

PACS: 68.55.Jk; 81.15.Gh; 71.55.Eq
Keywords: MOVPE; InP; InAs; Self-assembling

1. Introduction

Quantum dot structures in the form of coherent three-dimensional (3D) islands can be grown in situ by ''self-assembling'' in the two-dimensional (2D) layer + 3D island Stranski–Krastanow (SK) growth mode. Such SK-growth has been observed for a wide range of strained materials combinations, as for instance Ge_xSi_{1-x} on Si, $In_xGa_{1-x}As$ on GaAs, InP on $In_xGa_{1-x}P$/GaAs as well as the present combination InAs on InP [1–7]. The densities and sizes of such quantum dots are important parameters for device applications. Since the initiation mechanism of the 2D–3D transition is a nucleation step, the density, ρ, of stable islands in general follows the proportionality, $\rho \propto R/D$ [8]; where R is the deposition rate and D is the surface diffusion parameter. Due to the temperature dependence of D, the island density decreases with increasing temperature. The island sizes are in a first approximation defined by the amount of deposited material. Since the material is distributed over the stable growing nuclei, this distribution leads to the generally observed inverse relation between density and size [9].

In view of this general picture, the system of InAs dots on InP is exceptional due to the complexity of the dot formation mechanism associated with the chemical reactions at the InP/InAs interface. The

* Corresponding author. Tel.: +46-2227671; fax: +46-2223637.
E-mail address: magnus.borgstrom@ftf.lth.se (M. Borgström).

0169-4332/00/$ - see front matter
PII: S0169-4332(00)00517-1

reaction of AsH_3 with the InP surface, where P-atoms are easily replaced by As atoms, produces excess InAs [5,7]. The amount of excess InAs increases with temperature. This can lead to an uncommon temperature dependence where the density of InAs islands has been found to increase both when the temperature was decreased from 500°C to 480°C as well as when it was increased from 500°C to 520°C [6].

In this paper, we report on the effect of differently prepared InP surfaces on the formation of InAs islands. Moreover, we report on anomalous differences between island densities as InAs islands were grown either on semi-insulating or on n-type InP (001) substrates.

2. Experimental

The samples were grown in a low-pressure MOVPE system at 50 mbar using hydrogen as carrier gas and trimethyl-indium, trimethyl-gallium, arsine and phosphine as precursors. The process was controlled by a flow and pressure balanced ventilation/run system. We used a molar fraction of 5×10^{-4} for arsine and 1.5×10^{-2} for phosphine. The total gas flow in the reactor cell was about 6000 cm^3/min. As substrates, we used Fe-doped (SI) and Sn-doped (n^+) InP (001) (''epi-ready'' Sumitomo) wafers with a 0.2° misorientation towards the nearest $\langle 011 \rangle$ direction. Both substrate types were used simultaneously side by side in each growth run. A 200-nm thick InP buffer layer was grown initially at an elevated temperature of 650°C and growth rate of 1.2 ML/s which was gradually decreased to 0.3 ML/s during the growth of the buffer layer. The temperature was ramped down to 500°C, before deposition of the InAs dot material. For this ramp step, two different procedures were chosen: (i) the entire InP buffer layer was grown before the ramp and (ii) the last two thirds of the InP buffer layer was grown continuously during the ramp. In the first case, the well-defined terrace structure of the InP surface was preserved during cooling. In the second case, we left the step–flow growth mode and entered the 2D nucleation growth mode at approximately 530°C [10]. The subsequent deposition of nominally 1.5 or 2.4 ML InAs, during 5 and 8 s, respectively, at 500°C therefore took place either onto (i) a well-defined stepped structure with flat terraces or (ii) on a rather rough surface defined by numerous 2D islands on the terraces. After deposition of InAs, the surface was annealed under $H_2 + AsH_3$ for 12 s. Finally, the samples were either cooled down under $H_2 + AsH_3$, or capped by nominally 100 nm of InP. During the first 26-nm of cap layer growth, the growth temperature was linearly ramped to 600°C and was then maintained at this temperature during the remainder of the growth.

Conventional contact mode AFM was used to characterize the uncapped samples. The densities were evaluated by counting the islands on 2×2 μm^2 images.

The height distributions of the islands were evaluated by measuring the height of at least 100 islands and from these data, histograms were made. We take these height values as representative for the size of the islands. Neither the lateral extension nor the shape of the dots could be obtained with sufficient accuracy, due to severe convolution effects between the AFM-tip (with a nominal 50 nm tip-radius) and the sample.

Photoluminescence (PL) of the capped dot structures was carried out by Fourier Transform Spectroscopy, at different temperatures using an Ar-ion laser as excitation source with an excitation power of 50 mW. An InSb detector was used for detection.

3. Results and discussion

Fig. 1a,b shows the well-defined terrace structure of InP which developed during growth in the step–flow growth mode at a deposition temperature of 650°C. Both on InP:Sn as well as on InP:Fe, we counted about 34 steps along the diagonal of the 2×2 μm^2 AFM image, corresponding to the formation of 1 ML high steps on a surface of nominally 0.2° misorientation. Deposition of InAs dots at 500°C on such a stepped surface resulted in significantly different surface densities of $\rho = 0.5 \times 10^{10}$ cm^{-2} on InP:Sn and 1.7×10^{10} cm^{-2} on InP:Fe (c,d). The average height of the dots (e,f) was 10.3 nm on the Sn-doped and 8.9 nm on the Fe-doped InP. Fig. 2a,b shows AFM images of the InP surface which developed if the deposition continued while the tempera-

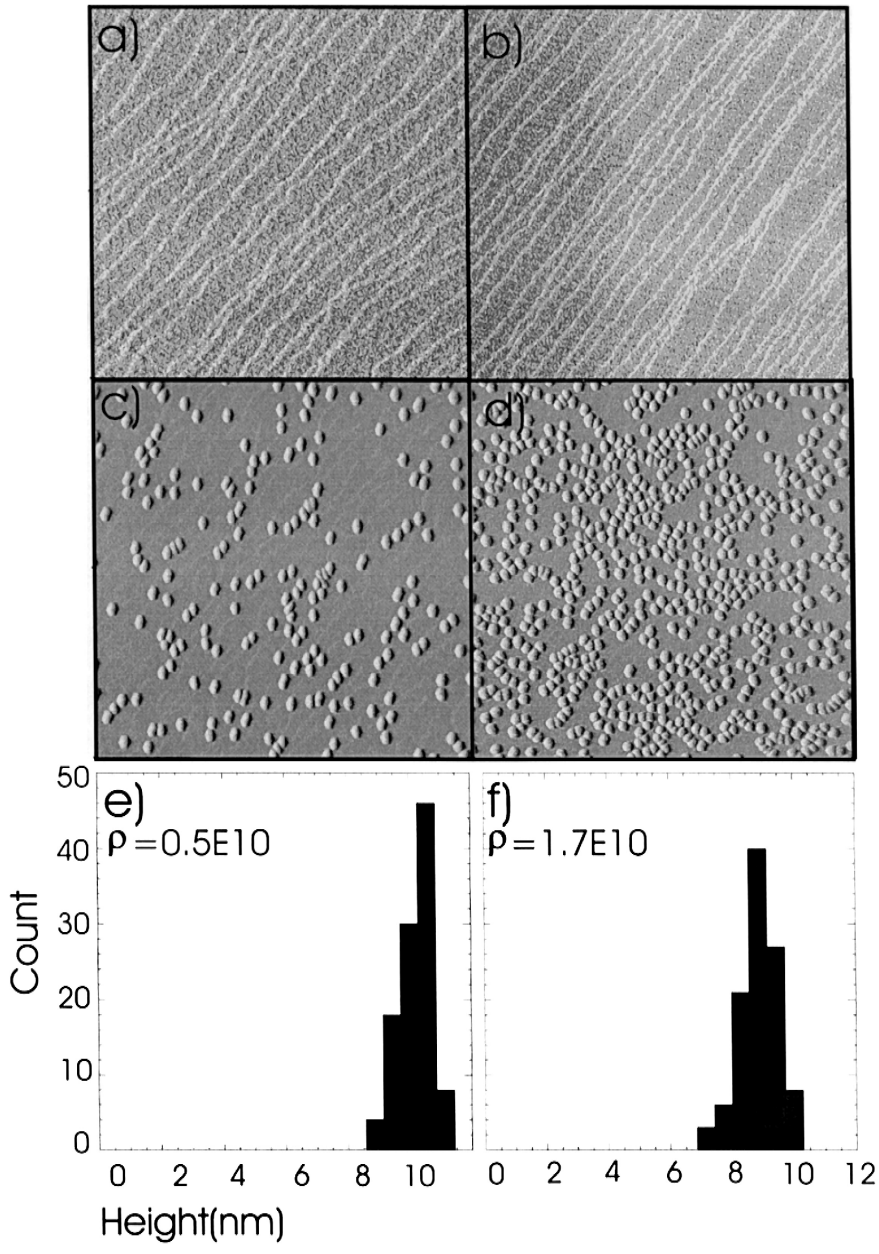

Fig. 1. AFM images (2×2 μm^2) of the terrace structure developed at 650°C on (a) InP/Sn and (b) InP/Fe. In (c) and (d), the InAs dots grown at 500°C on this stepped surface are shown, the corresponding height histograms are shown in (e) and (f).

ture was ramped down. Nucleation at the terraces resulted in a rough surface. Deposition of InAs dots at 500°C on such a rough surface resulted in generally higher, but also significantly differing surface dot densities of $\rho = 1.5 \times 10^{10}$ cm^{-2} on InP:Sn and 4.0×10^{10} cm^{-2} on InP:Fe (c,d). As a consequence of materials balancing and a higher density in comparison to the dots on a terraced surface (Fig. 1), the

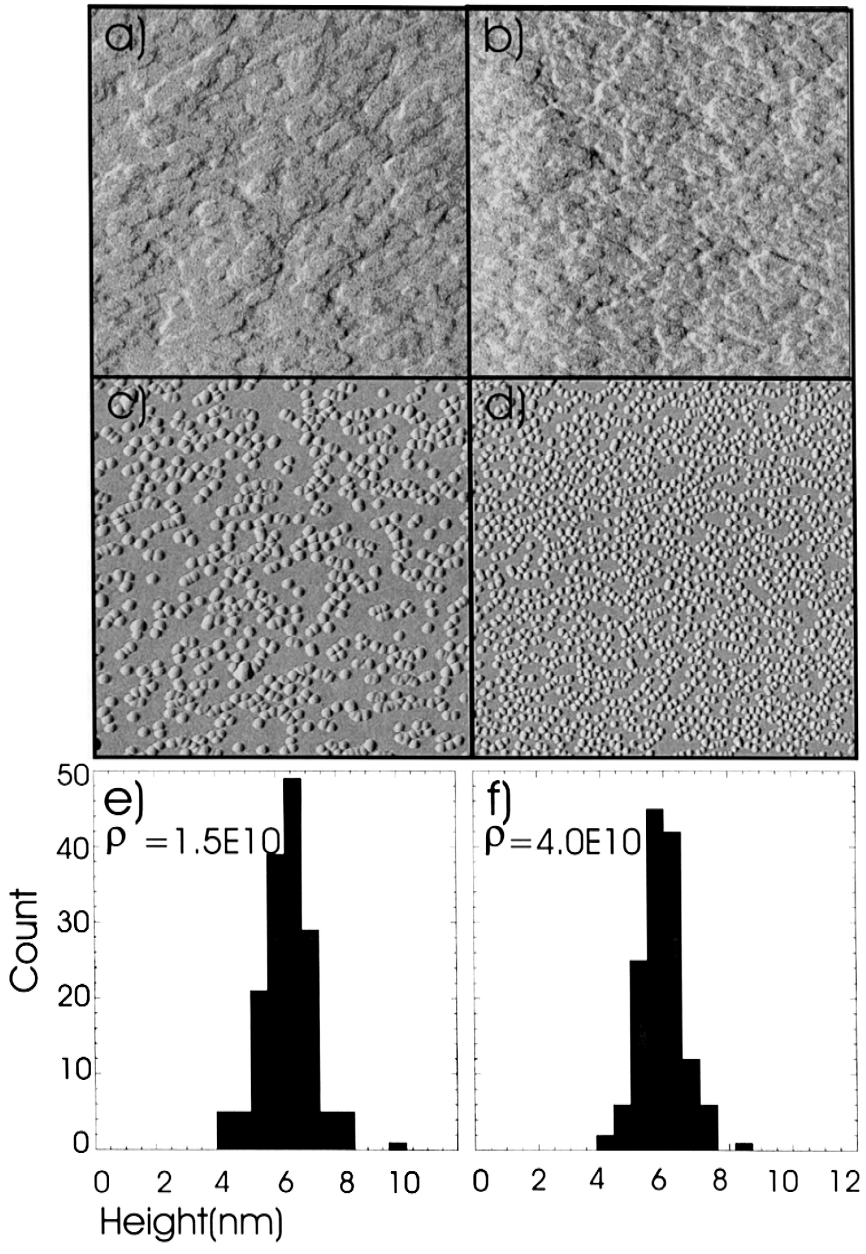

Fig. 2. AFM images (2×2 μm^2) of the surface structure developed by growth during cooling down to 500°C on (a) InP/Sn and (b) InP/Fe. In (c) and (d), the InAs dots grown on this surface are shown. The corresponding height histograms are shown in (e) and (f).

dots grown on such a rough surface were significantly smaller (e,f): 6.4 nm on the Sn-doped and 5.8 nm on the Fe-doped InP.

These differences in densities and sizes are also reflected in the PL spectra shown in Fig. 3. In the sample with the lower dot density on InP:Sn, we saw dot luminescence at 0.69 eV as well as wetting layer luminescence at 1.23 eV (corresponding to recombination in 2-ML thick quantum wells). The high-density sample on InP:Fe showed dot luminescence

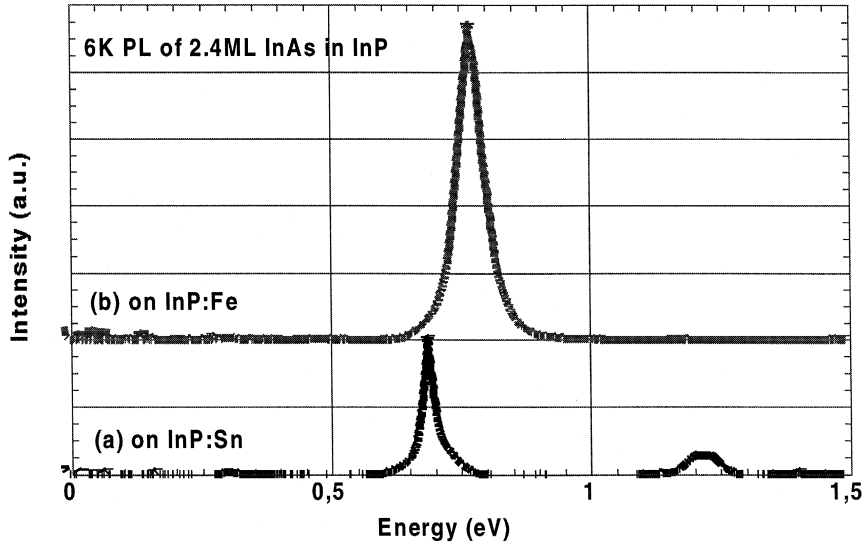

Fig. 3. PL (6 K) of 2.4 ML InAs grown on (a) InP/Sn and (b) InP/Fe substrates. The InAs dots were formed after growth of InP during the temperature ramp corresponding to the samples in Fig. 2.

at 0.77 eV only. We attributed the shift to higher energies to increased quantum confinement. This effect was not as pronounced in PL from dots with lower densities and larger sizes. With increasing average size of the dots, the difference in energy confinement due to a change in dot size decreases.

In order to explain the observed differences in dot densities grown on well-defined terrace structures in comparison to growth on rough surfaces, we obtain a clear picture by considering two effects. At first, a rough surface reduces the diffusion length of reactants and thereby creates more nucleation sites for dot formation. In fact, the area in Fig. 1c at higher magnification (not shown here) showed that the dots preferentially nucleated along the step edges, but only occasionally on top of the flat terraces. Secondly, a rough surface is more sensitive against As/P exchange reactions than the more inert terraced surface. This contributes to the production of excess InAs, available for dot formation in addition to the deposited InAs. In Fig. 4, PL spectra from 1.5 ML InAs on stepped surfaces are presented. The peaks for the Sn- and Fe-doped samples almost coincided, centred at 0.64 and 0.65 eV, respectively. The FWHM value, 21 meV at 5 K, was narrower than any line width reported so far for self-assembled dots of InAs in GaAs [11]. This we attribute to a high degree of homogeneity in dot sizes due to uniform dot nucleation almost only at the step edges. PL spectra from 2.4 ML InAs on stepped surfaces showed broad FWHM values of up to 70 meV. In

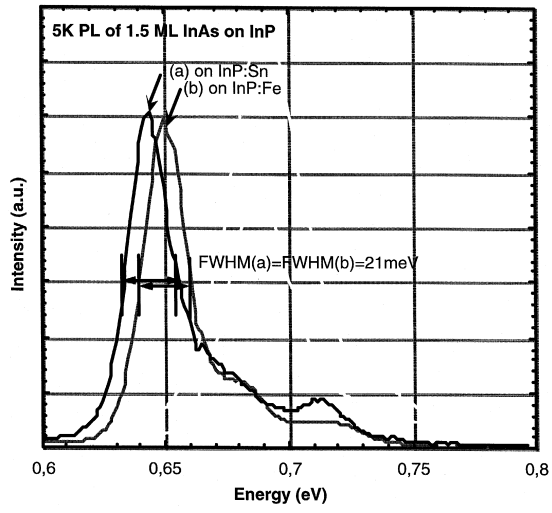

Fig. 4. PL (5 K) of 1.5 ML InAs grown on (a) InP/Sn and (b) InP/Fe terraced surfaces.

this case, we observe dot nucleation at the steps, as well as nucleation on the terraces.

We observed that the differently doped substrates have an influence on the dot densities and sizes. The ratios ρ (on Sn-doped)$/\rho$ (on Fe-doped) are 0.29 and 0.38 for dot densities on the terraced and the rough surface, respectively. These differences are primarily not explained by differences in the surface structure, as indicated by the very similar AFM images for the two types of substrates. Tentatively, we suggest that the differences may be caused by surface charges. There is a huge band-offset in the band structure at the InP/InAs interface and it is known that InAs surfaces tend to accumulate charges [12]. A higher charge accumulation in case of underlying n-type substrate in comparison to an underlying semi-insulating substrate could easily explain the observed differences: surface charges reduce the surface energy [13] and also affect the surface diffusion parameter D (charges affect the activation barrier E_d for site-hopping). We made the following experiment: we inserted a thin Si-doped layer (20 nm, $n \approx 2 \times 10^{18}$ cm^{-3}) during the buffer layer growth. This Si-doped layer had no noticeable effect on the step-structure before deposition of the InAs, as measured by AFM, but it reduced the differences by increasing the ratio ρ (on Sn-doped)$/\rho$ (on Fe-doped) to approximately 0.65. This result supports the assumption that charging effects could be responsible. However, preliminary attempts to find similar effects also for the system InAs/GaAs failed [14]. There are, in fact, some weak points in our tentative assumption of substrate-dependent charge-accumulations at the surface. At 500°C, the intrinsic carrier concentration is in the order of $n_i \times 10^{15}$ cm^{-3}, and this should level the carrier concentration differences to some degree. Another effect of the high temperature should be thermally activated escape of carriers from the thin InAs surface layer, which we are unable to quantify at the moment. Different substrate surface temperatures due to different thermal conductivity of the Sn- and Fe-doped substrates as reason for different dot densities have been taken into consideration, too. Therefore, the surface temperatures were measured by means of a pyrometer. No significant temperature difference between the differently doped substrates was observed. At the moment, we cannot rule out that completely different mechanisms, e.g. migration of the dopants towards the growing surface, contribute to the observed differences.

4. Conclusions

In conclusion, we have investigated the effect of substrate doping (InP:Sn and InP:Fe) and morphology of the InP (001) surface prior to InAs deposition on densities and sizes of self-assembled InAs quantum dots. The dots were grown at 500°C on either well-defined terrace surfaces with monolayer-high steps grown at 650°C in the step–flow growth mode, or on rougher InP surfaces prepared at a lower temperature of 500°C. The dot densities were found to vary between 0.5×10^{10} and 4.0×10^{10} cm^{-2}. The densities were significantly lower on terraced surfaces and on Sn-doped substrates in comparison to the rougher surface and Fe-doped substrates under otherwise identical growth conditions. This very broad scattering of densities indicates that InAs island formation on InP substrates is very sensitive to substrates and substrate preparation.

Acknowledgements

This work was performed within the Nanometer Structure Consortium at Lund University and was supported by grants from the Swedish National Board for Industrial and Technical Development (NUTEK), the Swedish Natural Science Research Council (NFR), the Swedish Foundation for Strategic Research (SSF) and the Swedish Research Council for Engineering Sciences (TFR).

References

[1] A. Ponchet, A.L. Corre, H. L'Haridon, B. Lambert, S. Salaün, Appl. Phys. Lett. 67 (1995) 1850.
[2] S. Fafard, Z. Wassilewski, J. McCaffrey, S. Raymond, S. Charbonneau, Appl. Phys. Lett. 68 (1996) 991.
[3] M.A. Cotta, C.A.C. Mendonca, E.A. Meneses, M.M.G.d. Carvalho, Surf. Sci. 388 (1997) 84.
[4] H. Marchand, P. Desjardins, S. Guillon, J.-E. Paultre, Z. Bougrioua, R.Y.-F. Yip, R.A. Masut, Appl. Phys. Lett. 71 (1997) 527.

[5] M. Taskinen, M. Sopanen, H. Lipsanen, J. Tulkki, T. Tuomi, J. Ahopelto, Surf. Sci. 376 (1997) 60.
[6] N. Carlsson, T. Junno, L. Montelius, M.-E. Pistol, L. Samuelson, W. Seifert, J. Cryst. Growth 191 (1998) 347.
[7] S. Yoon, Y. Moon, T.-W. Lee, E. Yoon, Appl. Phys. Lett. 74 (1999) 2029.
[8] J. Johansson, N. Carlsson, W. Seifert, Physica E 2 (1997) 667.
[9] W. Seifert, N. Carlsson, J. Johansson, M.-E. Pistol, L. Samuelson, J. Cryst. Growth 170 (1997) 39.
[10] M. Suhara, C. Nagao, H. Honji, Y. Miyamoto, K. Furuya, R. Takemura, J. Cryst. Growth 179 (1997) 18.
[11] I. Mukhametzanov, Z. Wei, R. Heitz, A. Madhukar, Appl. Phys. Lett. 75 (1999) 85.
[12] L.Ö. Olsson, C.B.M. Andersson, M.C. Håkansson, L. Ilver, U.O. Karlsson, Phys. Rev. Lett. 76 (1996) 3626.
[13] K. Choi, S.-J.L. Kang, H.M. Jang, N.M. Hwang, J. Cryst. Growth 172 (1997) 416.
[14] J. Johansson, M. Borgström, W. Seifert, unpublished results.